Phycobilisome breakdown effector NblD is required to maintain the cellular amino acid composition during nitrogen starvation

Vanessa Krauspe,[a] Stefan Timm,[b] Martin Hagemann,[b] Wolfgang R. Hess,[a,#]

[a]Genetics and Experimental Bioinformatics, Institute of Biology 3, Faculty of Biology, University of Freiburg, 79104 Freiburg, Germany

[b]Plant Physiology Department, Institute of Biosciences, University of Rostock, Rostock, 18059 Rostock, Germany;

Running Head: NblD affects metabolite pools

[#]Correspondence: Wolfgang R. Hess, wolfgang.hess@biologie.uni-freiburg.de

Keywords: amino acids, cyanobacteria, nitrogen starvation, photosynthesis, phycobilisomes, *Synechocystis* sp. PCC 6803, small proteins, stress response

Abstract

Nitrogen starvation induces a coordinated nitrogen-saving program in cyanobacteria. NblD is the 66-amino-acid effector of nitrogen-limitation-induced phycobilisome breakdown, which is believed to replenish the cellular amino acid pools. To address the physiological functions of NblD, the concentrations of amino acids, intermediates of the ornithine-ammonia cycle and several organic acids were measured during the response to nitrogen starvation in the cyanobacterium *Synechocystis* sp. PCC 6803 wild type and in an *nblD*-deletion strain. A characteristic signature of metabolite pool composition was identified, which shows that NblD-mediated phycobilisome degradation is required to maintain the cellular amino acid and organic acid pools during nitrogen starvation. Specific deviations from the wild type suggest wider-reaching effects that also affect such processes as redox homeostasis via glutathione and tetrapyrrole biosynthesis, both of which are linked to the strongly decreased glutamate pool, carbon fixation because the pool of 3-phosphoglyceric acid, the stable CO_2 fixation product of RubisCO, was also decreased, and transcriptional reprogramming via an enhanced concentration of 2-oxoglutarate, the metabolite coregulator of the NtcA transcription factor. The essential role played by NblD in metabolic homeostasis is consistent with the widespread occurrence of NblD throughout the cyanobacterial radiation and the previously observed strong positive selection for the *nblD* gene under fluctuating nitrogen supply.

Importance

Cyanobacteria play important roles in the global carbon and nitrogen cycles. In their natural environment, these organisms are exposed to fluctuating nutrient conditions.

Nitrogen starvation induces a coordinated nitrogen-saving program that includes the breakdown of nitrogen-rich photosynthetic pigments, particularly phycobiliproteins. NblD was recently identified as an effector of phycobilisome breakdown in cyanobacteria. In this study, we demonstrate that the NblD-mediated degradation of phycobiliproteins is needed to sustain cellular pools of soluble amino acids and other crucial metabolites. The essential role played by NblD in metabolic homeostasis explains why genes encoding this small protein are conserved in almost all members of cyanobacterial radiation.

Introduction

Nondiazotrophic cyanobacteria, such as the unicellular strain *Synechocystis* sp. PCC 6803 (hereafter designated *Synechocystis* 6803), depend on combined nitrogen (N) sources in their environment. These bacteria favor ammonia (NH_3 or NH_4^+) but can also utilize nitrate (NO_3^-) as an inorganic N source (1, 2). Under N-limited conditions, cells can start an acclimation program, manifested as chlorosis, and finally enter a dormant state (3–7). During chlorosis, N-rich pigments are degraded, predominantly the giant light-harvesting pigment-protein complexes, the phycobilisomes (3, 4, 8). The excess carbon (C) availability during chlorosis induces the accumulation of C reserves, particularly glycogen (9). The tricarboxylic acid (TCA) cycle intermediate 2-oxoglutarate (2-OG), which is primarily used as a C skeleton for ammonium incorporation by the glutamine synthetase/glutamine 2-OG aminotransferase (GS/GOGAT) cycle (10, 11), has been shown to serve as a cellular signal metabolite to report the relative N/C status (12–16). If ammonia assimilation via the GS/GOGAT cycle is slowed due to N deficiency, 2-OG is no longer converted and accumulates in the cyanobacterial cell. As a result, 2-OG can bind to the signal transduction protein PII (17, 18), thereby releasing PipX from the PipX/PII complex (14, 16). Free PipX can subsequently associate with and activate the global nitrogen transcription regulator NtcA. In *Synechocystis* 6803, NtcA directly controls 79 different genes after 4 h of N starvation (19). Depending on the location of the respective binding motifs, NtcA can either activate genes, especially those involved in nitrogen uptake and assimilation, or repress genes, as observed for the GS inhibition factors *gifA* and *gifB* (20). Two of the NtcA-activated genes in *Synechocystis* 6803 are *nblA1* and *nblA2* (*ssl0452* and *ssl0453*) (19), which encode small proteins that are critically important in N starvation-induced phycobilisome breakdown (21–24).

Phycobilisome breakdown in N-starved cyanobacteria is a tightly controlled process that is believed to fill cellular amino acid pools, compensating for the limited *de novo* nitrogen assimilation via the GS-GOGAT cycle. NblA1/A2 play essential roles in the coordinated process of phycobilisome degradation during N deprivation because corresponding mutants show a so-called nonbleaching phenotype (*nbl*), i.e., they retain their phycobilisomes under N-limiting conditions (21, 22). NblA proteins function as adaptors for the Clp protease by connecting the phycobiliproteins and the ClpC chaperone (23–26). Phycobilisome degradation can be generally divided into a rapid early phase, in which almost 50% of phycocyanin is recycled within 5 h, followed by a more sedate phase until only approximately 10% of the initial phycocyanin content is attained after 24 h of N deficiency (27). The degradation of the phycobilisome starts at the distal phycocyanin rods and extends to the allophycocyanin core, which is in proximity to the photosystems situated in the thylakoid membrane (26, 28). Previous studies showed that the inability to degrade phycobilisomes in the Δ*nblA1/A2* mutant affected the composition of amino acid pools during N starvation in a specific way in *Synechocystis* 6803 (29). These authors demonstrated that changes in the pool size of many amino acids during N starvation can be categorized as NblA1/A2-dependent (Gln, Glu, Gly, Ile, Leu, Met, Phe, Pro, Ser, Thr, Tyr, Val and the tripeptide glutathione important for redox homeostasis), while others were NblA1/A2-independent (Ala, Asn, Asp, Lys and Trp).

NblD has been recently identified as another small protein determined to be important for phycobilisome turnover because Δ*nblD* mutants do not bleach, even after several days under N starvation (30). NblD specifically binds to the phycocyanin beta subunit (CpcB) of phycobilisomes at an early time point of nitrogen depletion (30). However, the precise biochemical function of NblD remains to be determined. In this study, we

compared the metabolic composition of *Synechocystis* 6803 wild-type cells (WT) with a mutant deficient for NblD (Δ*nblD*) over a time course of N starvation. A characteristic signature in the composition of these metabolite pools was observed that supports the essential role played by NblD in the maintenance of cellular amino acid homeostasis during N starvation. Other deviations from the WT suggest wider-reaching effects, also affecting transcriptional reprogramming via an unusually high concentration of 2-OG, the metabolite coregulator of the NtcA transcription factor.

Results

In the present study, the amino acid pools and amounts of other important metabolites were compared in the *Synechocystis* 6803 wild type (WT) to an *nblD* deletion mutant (Δ*nblD*) under N-limited conditions. In contrast to the WT, cells of the Δ*nblD* strain do not exhibit any bleaching in the absence of a nitrogen source (30). Accordingly, we hypothesized that the soluble amino acid pools of Δ*nblD* cells may be exhausted more quickly than those of WT cells. This assumption was tested by metabolomics based on liquid chromatography mass spectrometry (LC-MS/MS) of three biologically independent samples for each WT and Δ*nblD*, taken before (+N condition), 3 h after and 24 h after the transfer into N-free BG11 medium. In total, 28 compounds, including almost all amino acids (Asn and Cys were below the detection limit), intermediates of the ornithine-ammonia cycle, and several organic acids, were quantified (see Table S1 for the LC-MS/MS raw data).

Samples obtained from the +N condition and 3 h after nitrogen removal showed no difference in pigmentation, whereas the WT samples showed pronounced bleaching after 24 h of N starvation, while the Δ*nblD* mutant did not (Fig. 1A and B). The

degradation of phycobilisomes resulted in transiently higher levels of total soluble amino acids in *Synechocystis* 6803 WT during N starvation (Fig. 2A, Table S2). The level of free amino acids increased from approximately 261 ng OD_{750}^{-1} ml^{-1} (± 32.4) under nitrogen-replete conditions (+N) by 65% on average after 3 h and approximately 27% (in relation to the starting value) after 24 h of N limitation (-N). In contrast, the Δ*nblD* mutant contained 335 ng OD_{750}^{-1} ml^{-1} (± 43.3) of free amino acids in the +N condition and remained at a similar level after 3 h. After 24 h after nitrogen removal, the amino acid content decreased dramatically by 70% to 75% in relation to the initial content in Δ*nblD* (Fig. 2A). Compared to the amino acid pool, the total amounts of other quantified metabolites, primarily organic acids, did not differ significantly between cells of the WT and Δ*nblD* (Fig. 2B), at least in the +N condition and after 24 h. The higher total amount after 3 h is mostly due to increased 2-OG, aconitate and citrate concentrations in the mutant (Fig. 5).

Despite the overall trend of a decreasing total amino acid pool in mutant Δ*nblD* compared to WT, the changes in the amounts of individual amino acids were not unidirectional (Fig. 3). Several amino acids showed similar trends in both WT and Δ*nblD* during nitrogen limitation, as was observed for Ala, Arg, Gln, His, Lys, and Trp. Three of them, Ala, Lys and Trp, have been previously reported to behave similarly in WT and Δ*nblA1/A2* mutants upon nitrogen depletion (29). The strongest deviation in the response to N starvation between the two strains was observed for Glu. The level of Glu did not decrease during the 24 h N starvation period in WT but decreased in mutant Δ*nblD* to approximately 17% of the initial value after 24 h of N starvation (Fig. 3). Glu is by far the most abundant soluble amino acid and serves as an amino group donor in the majority of transaminase reactions. Hence, the depletion of the Glu pool should have notable effects on the entire metabolism. Indeed, the lack of Glu extended

into the pool of reduced glutathione (GSH), which is the tripeptide γ-L-glutamyl-L-cysteinylglycine; the initial increase observed in the WT was lower in cells of the mutant Δ*nblD* and led after 24 h into N limitation to a significantly reduced amount (Fig. 3). GSH plays an important role as a reducing agent in all living cells and was found to be essential in the acclimation of *Synechocystis* 6803 to environmental and redox perturbations (31); hence, its depletion probably should have an impact on redox homeostasis in the mutant Δ*nblD*. Some amino acids, such as Gly, Pro, Ser, Thr and Val, exhibited transiently increased levels after 3 h in WT, which was not the case or was less pronounced in the mutant (Fig. 3). The branched chain amino acids Ile, Leu and Val share the same biosynthetic pathway, whereas Gly and Ser are closely linked to photorespiratory metabolism and can be interconverted by serine hydroxymethyltransferase (32). Phe and Thr exhibited increased levels in WT cells after 24 h of N starvation, while they returned to initial levels in Δ*nblD,* accumulating at values of less than 50% of the WT. Finally, the aromatic amino acid Tyr accumulated nearly 100-fold more in WT cells after 24 h of N starvation, whereas it remained at low levels in Δ*nblD* (Fig. 3). This finding is consistent with a previous analysis of *Synechocystis* 6803 WT after 24 h N starvation (29). Tyr represents approximately 5% of the amino acids stored in the phycobilisome (Fig. 4). The strong accumulation of Tyr in WT but not in Δ*nblD* suggests that it originated directly from phycobilisome degradation, assuming that in contrast to other amino acids, Tyr is not readily incorporated into the metabolism of N-starved cells.

Degradation of phycocyanin rods and their proteolytic recycling are assumed to contribute extensively to the amino acid pool in the cell, making those amino acids available to be incorporated into other proteins to acclimate towards nutrient limitation. From the phycobilisome core, up to six rod antennas radiate, each of which is built by

three hexameric discs connected with linker polypeptides CpcG and CpcC (33). One hexameric phycocyanin disc contains six subunits of each CpcA and CpcB. CpcA and CpcB are rich in Ala (14.2% and 17.4%, respectively), Gly (approximately 8%) and Leu (9.9% and 7%, respectively). In total, full phycobilisome turnover, including all linker proteins and allophycocyanin core, would provide substantial amounts of Ala (~14%), Leu, Gly (both ~8%), Ser, Val, Arg, and Asp (contributing 6-7% each to phycobilisome composition). If the degradation of phycobilisome proteins were to be directly used to fill the soluble amino acid pools in the cyanobacterial cell, one would expect the largest differences to be between WT and Δ*nblD* mutant cells in the amino acids dominating in the phycobilisomes. However, the relative amino acid proportions in the phycobilisome did not match the observed differences between the two strains with respect to specific amino acid pools (Fig. 4). For example, the amount of Ala was not significantly different between the two strains upon N starvation (Fig. 3), while for Leu, Gly, Ser and Val, significant differences were detected between WT and mutant under -N conditions. As mentioned above, besides Tyr the largest difference between WT and mutant Δ*nblD* was observed for the pool of Glu after 24 h of N starvation. Glu has an approximate 5% share in the composition of the phycobilisome proteins (Fig. 4). Therefore, it is likely that amino groups of abundant amino acids that become available upon phycobilisome degradation are utilized predominantly to stabilize the Glu pool via transaminase reactions, which is also consistent with the relatively lower amounts of 2-OG in WT compared to Δ*nblD* cells (Fig. 5).

In addition to proteinogenic amino acids, many additional metabolites could be quantified. For example, ornithine, the key metabolite of the ornithine-ammonia cycle, was clearly depleted in Δ*nblD* upon N starvation compared to WT (Fig. 5). The lower ornithine pool adds another point to the changed nitrogen homeostasis in

nonbleaching cells of *Synechocystis* 6803. This assumption was also supported by changes in the 2-OG pool, which was lower in WT than in mutant under all conditions, indicating a relatively more N-starved state of Δ*nblD* cells. Finally, the absence of NblD also affected C fixation because the pool of 3-phosphglyceric acid (3PGA), the stable CO_2 fixation product of RubisCO, was also decreased in +N and at 24 h at -N. Excess 3PGA can be used to produce glycogen, which is highly accumulating in N-starved cells during chlorosis (34). Otherwise, some 3PGA is diverted into the direction of lower glycolysis and the TCA cycle, which is primarily regulated by PirC (35). In contrast to the decreased flow into the oxidative branch, the reductive branch of the TCA cycle seemed to be less affected, since the pool of malate was similar in cells of the mutant and the WT (Fig. 5). However, succinate was clearly lowered in Δ*nblD* after 3 h under N limitation, probably due to enhanced consumption of succinate by the respiratory chain. In the mutant cells, the succinate pool stabilized at a similar quantity as was observed in WT cells under prolonged N depletion. Taken together, the metabolic changes observed in this study enabled us to conclude that the absence of NblD had a broad impact on primary metabolism.

Discussion

NblD is involved in the disassembly of phycobilisomes during acclimation to N starvation, targeting CpcB (30). The Δ*nblD* mutant has a nonbleaching phenotype, i.e., phycobilisomes are retained (see Fig. 1). In the present study, we analyzed the effects of the absence of NblD on the amino acid and organic acid pools in a Δ*nblD* deletion mutant. The observed differences between Δ*nblD* and WT in the amino acid pools were similar to those described for the Δ*nblA1/A2* mutant (29) but were not identical, despite the roles played by both types of proteins in phycobilisome degradation.

The most abundant phycobilisome proteins are CpcA and CpcB, which are rich in Ala, Gly, Leu, Val and Tyr. Accordingly, the pools of these amino acids were expected to increase early during N starvation-induced phycobilisome degradation in the WT. This change was clearly observed for Tyr, whereas the changes in the other amino acids were less pronounced between WT and Δ*nblD* cells. This phenomenon was particularly noted for Ala, the most frequent amino acid in phycocyanin, because it showed a similar pool change in WT and mutant cells, suggesting its increase resulted from synthesis instead. Ala biosynthesis is derived from the transamination of pyruvate and Glu by alanine dehydrogenase (*sll1682*) or by serine-pyruvate aminotransferase using pyruvate and Ser. Therefore, Ala is directly linked to the metabolic pathways of Ser, Gly and Thr, as well as to primary C metabolism, via pyruvate. Indeed, in *Synechococcus elongatus* PCC 7942, alanine dehydrogenase was found to be required for correct phycobilisome degradation during N starvation, resulting in lower *nblA* transcription if the gene for dehydrogenase was deleted (36).

Our results support the hypothesis that amino acid pools are regulated independently of phycobilisome degradation by NblA1/A2 and NblD because the cells maintain distinct amino acid pool homeostasis involving many transaminase reactions, primarily using the amino groups from the released phycobilisome constituents. Furthermore, such amino acids as Ala, Asp and Lys might originate from the breakdown of several other proteins (29). Hence, even though NblA1/NblA2- and NblD-assisted phycobilisome degradation represents the most obvious protein degradation process due to visible pigment changes, additional changes in the proteome likely contribute to the recycling of amino acids during acclimation to N starvation.

Amino acids are best known as the building blocks of proteins. However, additional functions have been assigned to some amino acids, such as the Glu/Gln pair (Fig. 5).

In addition to the role played by Glu as an amino group donor in transaminase reactions, Glu serves as the precursor of tetrapyrrole synthesis, leading to cytochromes and especially chlorophylls in cyanobacteria, green algae and plants upon activation by binding to its cognate $tRNA^{glu}$ (37–39). This C5 pathway is the sole biosynthetic pathway for tetrapyrrole biogenesis in *Synechocystis* 6803 (40, 41). Moreover, Glu is used as a signaling molecule in green algae, mosses and higher plants sensed by the PII protein (42). In contrast, in several gram-negative bacteria, Gln serves as a signaling molecule for N availability (reviewed by Forchhammer, 2013 (43)). More recently, it was observed that Gln also exhibits a signaling function in *Synechocystis* 6803 and other cyanobacteria via interaction with the GlnA riboswitch governing the expression of *gifB* mRNA (44).

In contrast to gram-negative bacteria, cyanobacteria use the TCA cycle intermediate 2-OG to sense the C/N status. 2-OG is the regulatory co-factor of NtcA and of PII. 2-OG accumulates in the absence of N and is bound by PII (17, 18), inducing the release of PipX from the PipX/PII complex (14, 16) and promoting the formation of the NtcA-PipX complex. In addition, NtcA binds 2-OG directly (13, 45). Both processes lead to the activation of NtcA. Conversely, if a N source is available, 2-OG is converted via the GS/GOGAT cycle to Glu, and its levels are low, as is the activity of NtcA. In addition, the decrease in 2-OG is associated with C limitation and activates transcription factors to upregulate genes involved in the cyanobacterial inorganic C-concentrating mechanism (46, 47).

Hence, the increase in 2-OG in the WT observed during N starvation should represent a pronounced signal for activation of NtcA, and indeed, the transcriptional units within the NtcA regulon become strongly differentially regulated during this condition (30). Notably, there is an NtcA motif in the promotor region of the *nblD* gene itself (48),

consistent with its role in N-limited conditions. However, compared to WT, we observed that 2-OG increased even more in Δ*nblD* and at every sampling point, including the +N condition (Fig. 5). Because of the function of 2-OG as the main cellular indicator metabolite to report C/N homeostasis (12–16), increased 2-OG levels therefore clearly indicated a reduced ammonia assimilating capacity of mutant Δ*nblD* already under N replete conditions. The likely reduced use of 2-OG in the GS/GOGAT cycle was supported by the observation that the levels of citrate and aconitate, precursors of 2-OG in the oxidative branch in the open cyanobacterial TCA cycle, were lowered in Δ*nblD* (Fig. 5). If the flux into the GS/GOGAT cycle would be similar, this decrease should extend into the 2-OG pool; however, its increase indicates reduced 2-OG utilization in mutant cells, whereas 2-OG was extensively used in WT to replenish the Glu pool.

The higher 2-OG level in Δ*nblD* than in the WT cells already in the +N condition can likely explain the stimulation of the NtcA regulon in Δ*nblD* observed during the previous transcriptome analysis. For example, the mRNA levels of NtcA-regulated *nblA1A2*, *gifA* and *gifB* were enhanced in Δ*nblD* under +N conditions (30). At 3 h after the induction of nitrogen starvation, *nblA1A2* mRNA levels were more strongly induced compared to the wild type ($\log_2$FC of +4.28 and +4.09 in Δ*nblD* and +3.71 and +3.47 in the wild type), while *gifA* and *gifB* were more strongly reduced (for both genes, $\log_2$FC of -4.7 in Δ*nblD* and -2.4 in the wild type control) (30). The differences observed between the mutant and WT in the +N condition indicated that NblD, in addition to its prominent function during N starvation, also plays some role under N-replete conditions. This function of NblD could be related to the remodeling of phycobilisome composition, size and number per thylakoid membrane or to the turnover of phycobilisomes occurring under N-replete conditions.

Materials and Methods

Cultivation conditions and sampling for metabolite analysis

Synechocystis 6803 PCC-M was used as the wild type and background for the construction of mutants. *NblD* knockout mutants were generated by homologous replacement of the *nblD* coding sequence with a kanamycin resistance cassette (*nptII*) (30).

Strains were maintained in copper-free BG11 supplemented with 20 mM TES PUFFERAN®, pH 7.5, under continuous white light of 50 µmol photons m^{-2} s^{-1} at 30°C. Wild-type and Δ*nblD* cultures were grown to OD ~0.8 in triplicate without antibiotics before cells were pelleted by centrifugation (3,210 × *g*, 8 minutes, room temperature), washed three times in BG11 without N and resuspended in BG11 lacking a N source. After three and 24 h of incubation in N-limited conditions, the OD was recorded, and 2 ml of each culture was collected by centrifugation (9,000 × *g*, 1 minute, room temperature) and immersed in liquid nitrogen. As controls, samples were also obtained before N removal (+N). For extraction, 630 µl methanol containing carnitine (internal standard, 1 µg per extraction) was added, mixed for one minute and incubated for 5 minutes in a sonic water bath. After another 15 minutes of shaking at room temperature, 400 µl of chloroform was added, and the sample was incubated at 37°C for 5 minutes. Next, 800 µl ROTISOLV® LC-MS grade H_2O (Roth) was added, and the sample was mixed thoroughly. Precipitation was enabled by storage at -20°C for at least 2 h, and phase separation was subsequently achieved by centrifugation for 5 minutes at room temperature (16,800 × *g*). The upper polar phase was collected and dried in a speed vac for 30 minutes followed by lyophilization overnight. A mock

sample without any culture was subjected to the same treatments as the other samples.

Metabolite analysis

Absolute metabolite contents were quantified on a high-performance liquid chromatograph mass spectrometer LCMS-8050 system (Shimadzu) as described previously (49). Dried samples were dissolved in 200 µl LCMS grade water and filtered through 0.2-mm filters (Omnifix-F, Braun, Germany), and 4 µl of the cleared supernatant was separated on a pentafluorophenylpropyl column (Supelco Discovery HS FS, 3 mm, 150 3 2.1 mm).

The compounds were identified and quantified using the multiple reaction monitoring (MRM) values given in the LC-MS/MS method package and the LabSolutions software package (Shimadzu). Authentic standard substances (Merck) at varying concentrations were used for calibration, and peak areas were normalized to signals of the internal standard (carnitine). The data were further normalized to the OD_{750} measured for each sample and corrected by signals obtained from the mock sample. The raw data are given in Table S1, statistical evaluations in Table S3.

Funding

We appreciate the support by the Deutsche Forschungsgemeinschaft (DFG, German Research Foundation) to WRH through the graduate school MeInBio - 322977937/GRK2344 and to WRH and MH through the priority program “Small Proteins in Prokaryotes, an Unexplored World” SPP 2002 (grants DFG HE2544/12-2 and DFG HA2002/22-2). The LC-MS equipment at the University of Rostock was financed through the Hochschulbauförderungsgesetz program (GZ: INST 264/125-1 FUGG to MH).

Conflict of interest statement

The authors declare that they have no conflicts of interest.

Author Contributions

WRH designed the project and secured funding. VK constructed and cultivated strains, MH and ST measured metabolite concentrations. VK, MH and WRH wrote the manuscript with input from all authors.

References

1. Muro-Pastor MI, Reyes JC, Florencio FJ. 2005. Ammonium assimilation in cyanobacteria. Photosynth Res 83:135–150.
2. Herrero A, Muro-Pastor AM, Flores E. 2001. Nitrogen control in cyanobacteria. J Bacteriol 183:411–425.
3. Allen MM, Smith AJ. 1969. Nitrogen chlorosis in blue-green algae. Archiv für Mikrobiologie 69:114–120.
4. Görl M, Sauer J, Baier T, Forchhammer K. 1998. Nitrogen-starvation-induced chlorosis in *Synechococcus* PCC 7942: adaptation to long-term survival. Microbiology 144:2449–2458.
5. Krasikov V, Aguirre von Wobeser E, Dekker HL, Huisman J, Matthijs HC. 2012. Time-series resolution of gradual nitrogen starvation and its impact on photosynthesis in the cyanobacterium *Synechocystis* PCC 6803. Physiol Plant 145:426–439.
6. Sauer J, Schreiber U, Schmid R, Völker U, Forchhammer K. 2001. Nitrogen starvation-induced chlorosis in *Synechococcus* PCC 7942. Low-level photosynthesis as a mechanism of long-lerm survival. Plant Physiol 126:233–243.
7. Spät P, Klotz A, Rexroth S, Maček B, Forchhammer K. 2018. Chlorosis as a developmental program in cyanobacteria: The proteomic fundament for survival and awakening. Mol Cell Proteomics 17:1650–1669.
8. Collier JL, Grossman AR. 1992. Chlorosis induced by nutrient deprivation in *Synechococcus* sp. strain PCC 7942: not all bleaching is the same. J Bacteriol 174:4718–4726.
9. Gründel M, Scheunemann R, Lockau W, Zilliges Y. 2012. Impaired glycogen synthesis causes metabolic overflow reactions and affects stress responses in the cyanobacterium *Synechocystis* sp. PCC 6803. Microbiology 158:3032–3043.
10. Meeks JC, Wolk CP, Lockau W, Schilling N, Shaffer PW, Chien WS. 1978. Pathways of assimilation of $^{[13N]}N_2$ and $^{13}NH_4^+$ by cyanobacteria with and without heterocysts. J Bacteriol 134:125–130.
11. Florencio FJ, García-Domínguez M, Martín-Figueroa E, Crespo JL, Navarro F, Muro-Pastor MI, Reyes JC. 1998. Ammonium assimilation in cyanobacteria. The

regulation of the GS-GOGAT pathway, p. 3607–3612. *In* Garab, G (ed.), Photosynthesis: Mechanisms and Effects: Volume I–V: Proceedings of the XIth International Congress on Photosynthesis, Budapest, Hungary, August 17–22, 1998. Springer Netherlands, Dordrecht.

12. Vázquez-Bermúdez MF, Herrero A, Flores E. 2002. 2-Oxoglutarate increases the binding affinity of the NtcA (nitrogen control) transcription factor for the *Synechococcus glnA* promoter. FEBS Lett 512:71–74.
13. Tanigawa R, Shirokane M, Maeda S -i., Omata T, Tanaka K, Takahashi H. 2002. Transcriptional activation of NtcA-dependent promoters of *Synechococcus* sp. PCC 7942 by 2-oxoglutarate *in vitro*. Proc Natl Acad Sci U S A 99:4251–4255.
14. Espinosa J, Forchhammer K, Burillo S, Contreras A. 2006. Interaction network in cyanobacterial nitrogen regulation: PipX, a protein that interacts in a 2-oxoglutarate dependent manner with PII and NtcA. Mol Microbiol 61:457–469.
15. Espinosa J, Rodriguez-Mateos F, Salinas P, Lanza VF, Dixon R, de la Cruz F, Contreras A. 2014. PipX, the coactivator of NtcA, is a global regulator in cyanobacteria. Proc Natl Acad Sci U S A 111:E2423–E2430.
16. Forcada-Nadal A, Llácer JL, Contreras A, Marco-Marín C, Rubio V. 2018. The PII-NAGK-PipX-NtcA regulatory axis of cyanobacteria: A tale of changing partners, allosteric effectors and non-covalent interactions. Front Mol Biosci 5:91.
17. Forchhammer K. 2004. Global carbon/nitrogen control by PII signal transduction in cyanobacteria: from signals to targets. FEMS Microbiol Rev 28:319–333.
18. Forchhammer K. 2008. PII signal transducers: novel functional and structural insights. Trends Microbiol 16:65–72.
19. Giner-Lamia J, Robles-Rengel R, Hernández-Prieto MA, Muro-Pastor MI, Florencio FJ, Futschik ME. 2017. Identification of the direct regulon of NtcA during early acclimation to nitrogen starvation in the cyanobacterium *Synechocystis* sp. PCC 6803. Nucleic Acids Res 45:11800–11820.
20. García-Domínguez M, Reyes JC, Florencio FJ. 2000. NtcA represses transcription of *gifA* and *gifB*, genes that encode inhibitors of glutamine synthetase type I from *Synechocystis* sp. PCC 6803. Mol Microbiol 35:1192–1201.

21. Collier JL, Grossman AR. 1994. A small polypeptide triggers complete degradation of light-harvesting phycobiliproteins in nutrient-deprived cyanobacteria. EMBO J 13:1039–1047.
22. Baier K, Nicklisch S, Grundner C, Reinecke J, Lockau W. 2001. Expression of two *nblA*-homologous genes is required for phycobilisome degradation in nitrogen-starved *Synechocystis* sp. PCC6803. FEMS Microbiol Lett 195:35–39.
23. Karradt A, Sobanski J, Mattow J, Lockau W, Baier K. 2008. NblA, a key protein of phycobilisome degradation, interacts with ClpC, a HSP100 chaperone partner of a cyanobacterial Clp protease. J Biol Chem 283:32394–32403.
24. Baier A, Winkler W, Korte T, Lockau W, Karradt A. 2014. Degradation of phycobilisomes in *Synechocystis* sp. PCC6803: evidence for essential formation of an NblA1/NblA2 heterodimer and its codegradation by a Clp protease complex. J Biol Chem 289:11755–11766.
25. Nguyen AY, Bricker WP, Zhang H, Weisz DA, Gross ML, Pakrasi HB. 2017. The proteolysis adaptor, NblA, binds to the N-terminus of β-phycocyanin: Implications for the mechanism of phycobilisome degradation. Photosyn Res 132:95–106.
26. Sendersky E, Kozer N, Levi M, Moizik M, Garini Y, Shav-Tal Y, Schwarz R. 2015. The proteolysis adaptor, NblA, is essential for degradation of the core pigment of the cyanobacterial light-harvesting complex. Plant J 83:845–852.
27. Elmorjani K, Herdman M. 1987. Metabolic control of phycocyanin degradation in the cyanobacterium *Synechocystis* PCC 6803: a glucose effect. Microbiology 133:1685–1694.
28. Hu P-P, Hou J-Y, Xu Y-L, Niu N-N, Zhao C, Lu L, Zhou M, Scheer H, Zhao K-H. 2020. The role of lyases, NblA and NblB proteins and bilin chromophore transfer in restructuring the cyanobacterial light-harvesting complex. Plant J 102:529–540.
29. Kiyota H, Hirai MY, Ikeuchi M. 2014. NblA1/A2-dependent homeostasis of amino acid pools during nitrogen starvation in *Synechocystis* sp. PCC 6803. Metabolites 4:517–531.
30. Krauspe V, Fahrner M, Spät P, Steglich C, Frankenberg-Dinkel N, Maček B, Schilling O, Hess WR. 2021. Discovery of a novel small protein factor involved in the coordinated degradation of phycobilisomes in cyanobacteria. Proc Natl Acad Sci U S A 118:e2012277118.

31. Cameron JC, Pakrasi HB. 2010. Essential role of glutathione in acclimation to environmental and redox perturbations in the cyanobacterium *Synechocystis* sp. PCC 6803. Plant Physiol 154:1672–1685.
32. Eisenhut M, Kahlon S, Hasse D, Ewald R, Lieman-Hurwitz J, Ogawa T, Ruth W, Bauwe H, Kaplan A, Hagemann M. 2006. The plant-like C2 glycolate cycle and the bacterial-like glycerate pathway cooperate in phosphoglycolate metabolism in cyanobacteria. Plant Physiol 142:333–342.
33. Arteni AA, Ajlani G, Boekema EJ. 2009. Structural organisation of phycobilisomes from *Synechocystis* sp. strain PCC6803 and their interaction with the membrane. Biochim Biophys Acta 1787:272–279.
34. Klotz A, Georg J, Bučinská L, Watanabe S, Reimann V, Januszewski W, Sobotka R, Jendrossek D, Hess WR, Forchhammer K. 2016. Awakening of a dormant cyanobacterium from nitrogen chlorosis reveals a genetically determined program. Curr Biol 26:2862–2872.
35. Orthwein T, Scholl J, Spät P, Lucius S, Koch M, Macek B, Hagemann M, Forchhammer K. 2021. The novel PII-interactor PirC identifies phosphoglycerate mutase as key control point of carbon storage metabolism in cyanobacteria. Proc Natl Acad Sci U S A 118:e2019988118.
36. Lahmi R, Sendersky E, Perelman A, Hagemann M, Forchhammer K, Schwarz R. 2006. Alanine dehydrogenase activity is required for adequate progression of phycobilisome degradation during nitrogen starvation in *Synechococcus elongatus* PCC 7942. J Bacteriol 188:5258–5265.
37. Wang W-Y, Gough SP, Kannangara CG. 1981. Biosynthesis of Δ-aminolevulinate in greening barley leaves IV. Isolation of three soluble enzymes required for the conversion of glutamate to Δ-aminolevulinate. Carlsberg Res Commun 46:243.
38. Kannangara CG, Gough SP, Oliver RP, Rasmussen SK. 1984. Biosynthesis of Δ-aminolevulinate in greening barley leaves VI. Activation of glutamate by ligation to RNA. Carlsberg Res Commun 49:417.
39. Schön A, Krupp G, Gough S, Berry-Lowe S, Kannangara CG, Söll D. 1986. The RNA required in the first step of chlorophyll biosynthesis is a chloroplast glutamate tRNA. Nature 322:281–284.

40. O'Neill GP, Peterson DM, Schön A, Chen MW, Söll D. 1988. Formation of the chlorophyll precursor delta-aminolevulinic acid in cyanobacteria requires aminoacylation of a tRNAGlu species. J Bacteriol 170:3810–3816.
41. Rieble S, Beale SI. 1988. Transformation of glutamate to delta-aminolevulinic acid by soluble extracts of *Synechocystis* sp. PCC 6803 and other oxygenic prokaryotes. J Biol Chem 263:8864–8871.
42. Chellamuthu V-R, Ermilova E, Lapina T, Lüddecke J, Minaeva E, Herrmann C, Hartmann MD, Forchhammer K. 2014. A widespread glutamine-sensing mechanism in the plant kingdom. Cell 159:1188–1199.
43. Forchhammer K. 2007. Glutamine signalling in bacteria. Front Biosci 12:10–2741.
44. Klähn S, Bolay P, Wright PR, Atilho RM, Brewer KI, Hagemann M, Breaker RR, Hess WR. 2018. A glutamine riboswitch is a key element for the regulation of glutamine synthetase in cyanobacteria. Nucleic Acids Res 46:10082–10094.
45. Zhao M-X, Jiang Y-L, He Y-X, Chen Y-F, Teng Y-B, Chen Y, Zhang C-C, Zhou C-Z. 2010. Structural basis for the allosteric control of the global transcription factor NtcA by the nitrogen starvation signal 2-oxoglutarate. Proc Natl Acad Sci U S A 107:12487–12492.
46. Jiang Y-L, Wang X-P, Sun H, Han S-J, Li W-F, Cui N, Lin G-M, Zhang J-Y, Cheng W, Cao D-D, Zhang Z-Y, Zhang C-C, Chen Y, Zhou C-Z. 2018. Coordinating carbon and nitrogen metabolic signaling through the cyanobacterial global repressor NdhR. Proc Natl Acad Sci U S A 115:403–408.
47. Klähn S, Orf I, Schwarz D, Matthiessen JKF, Kopka J, Hess WR, Hagemann M. 2015. Integrated transcriptomic and metabolomic characterization of the low-carbon response using an *ndhR* mutant of *Synechocystis* sp. PCC 6803. Plant Physiol 169:1540.
48. Baumgartner D, Kopf M, Klähn S, Steglich C, Hess WR. 2016. Small proteins in cyanobacteria provide a paradigm for the functional analysis of the bacterial micro-proteome. BMC Microbiol 16:285.
49. Reinholdt O, Schwab S, Zhang Y, Reichheld J-P, Fernie AR, Hagemann M, Timm S. 2019. Redox-regulation of photorespiration through mitochondrial thioredoxin o1. Plant Physiol 181:442–457.

Figures

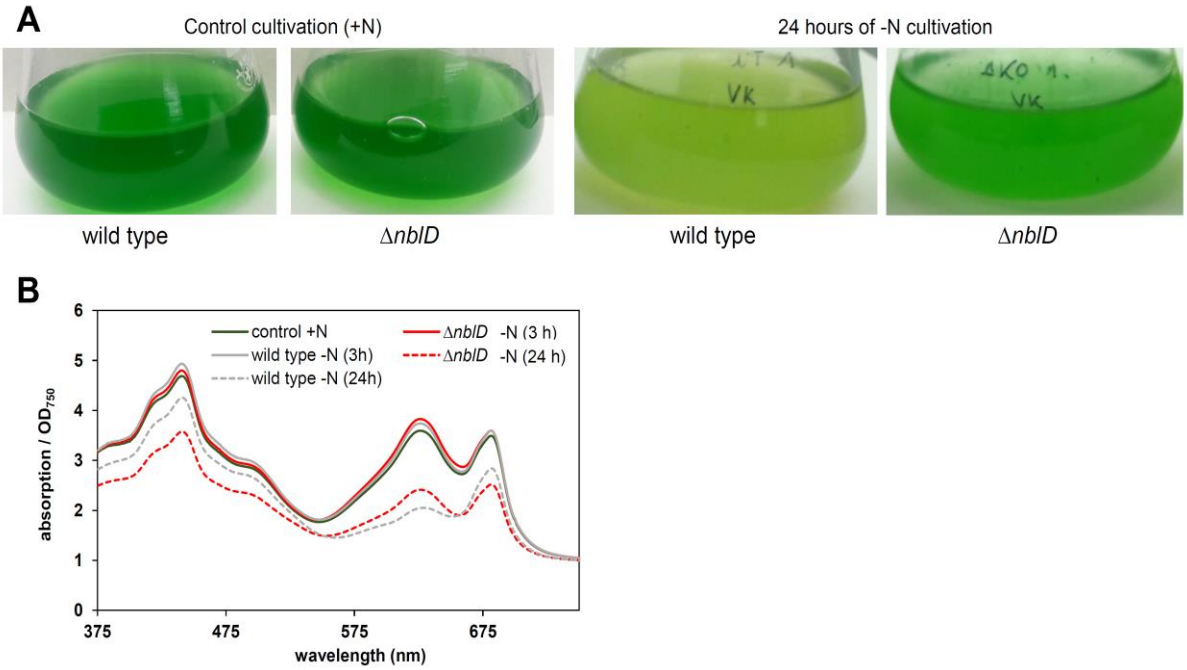

Figure 1. Response of the *Synechocystis* 6803 WT and Δ*nblD* mutant during the response to nitrogen starvation. **A.** Phenotype under nitrogen-replete (+N) conditions and after 24 h of nitrogen depletion (-N). **B.** Spectrometric measurements of cultures normalized to OD_{750}.

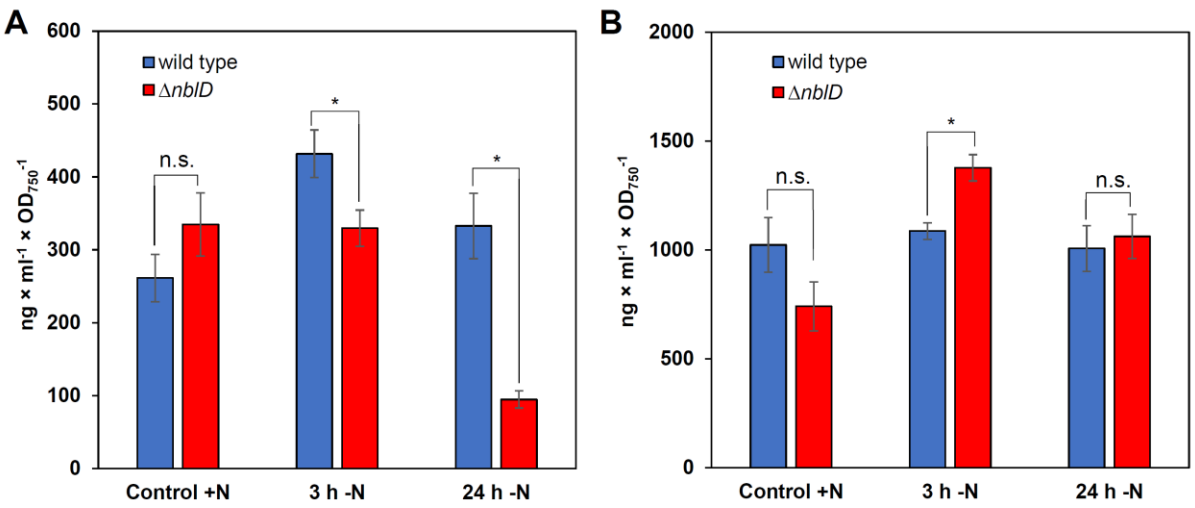

Figure 2. **A.** Total soluble amino acid content and **B.** total soluble metabolite content (nonproteinogenic amino acids and important intermediates) of wild-type (blue) and Δ*nblD* (red) cultures in nitrogen-replete (+N) and nitrogen-depleted BG11 (-N) after 3 h and 24 h. For each time point and strain, triplicates were measured, and significance ($p < 0.05$) was calculated by t-test; n.s. = not significant. The raw data are given in Table S2.

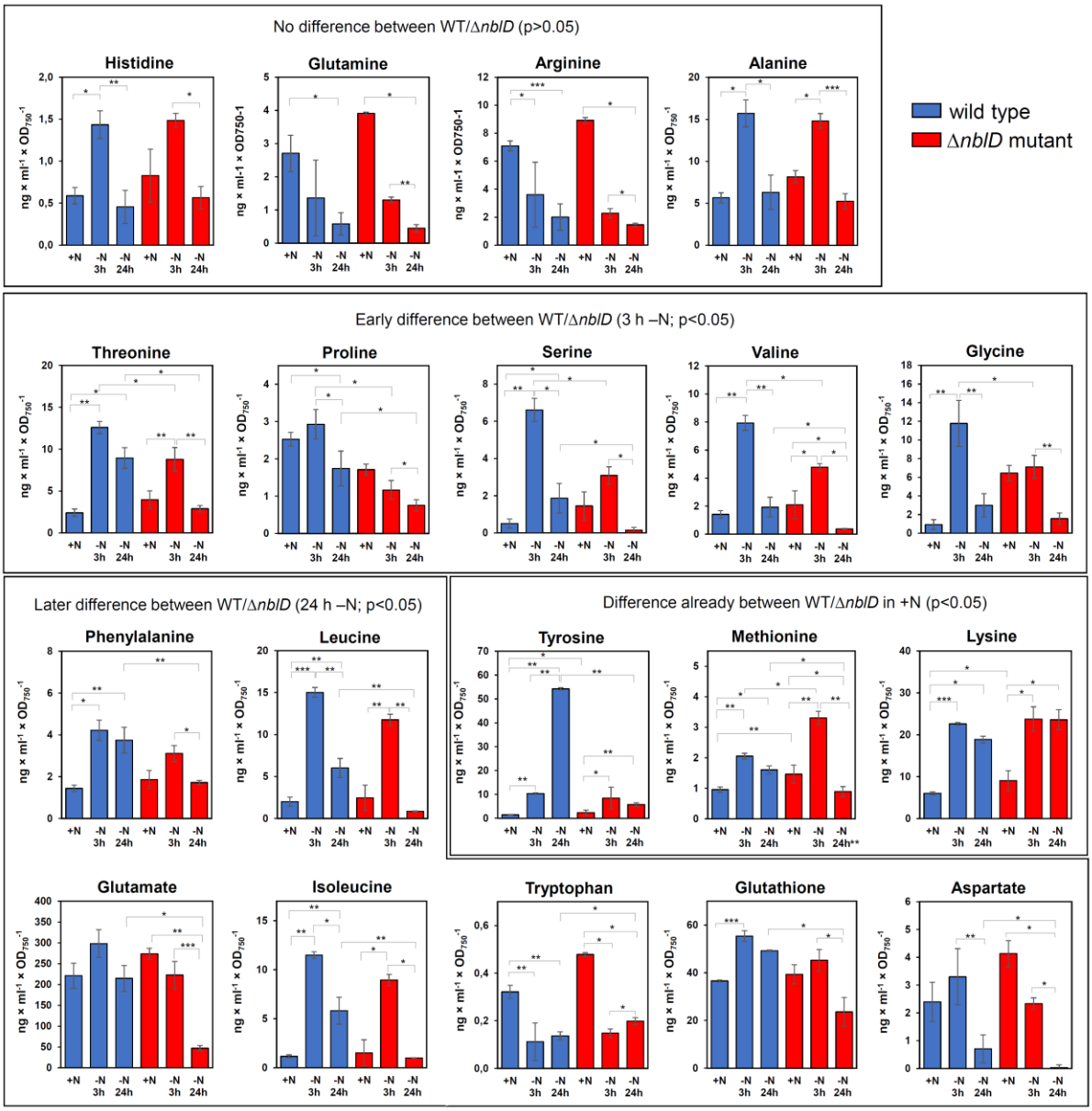

Figure 3. Development of amino acid content (in nanogram × ml^{-1} × OD_{750}^{-1}) in WT (blue) and Δ*nblD* mutant (red) in nitrogen replete (+N) and nitrogen deplete (-N) medium after 3 h and 24 h. Amino acids are grouped together according to the observed differences between wild type and mutant as follows: Difference already observed in +N conditions; no difference between strains; early difference (after 3 h); later differences (24 h). Significance was calculated with a two-sample t-test with unequal variance (Welch's t-test; $p < 0.05$ = *; $p < 0.01$ = ** and $p < 0.001$ = ***) for the development in each strain and between the strains at corresponding time points (see Table S3 for details).

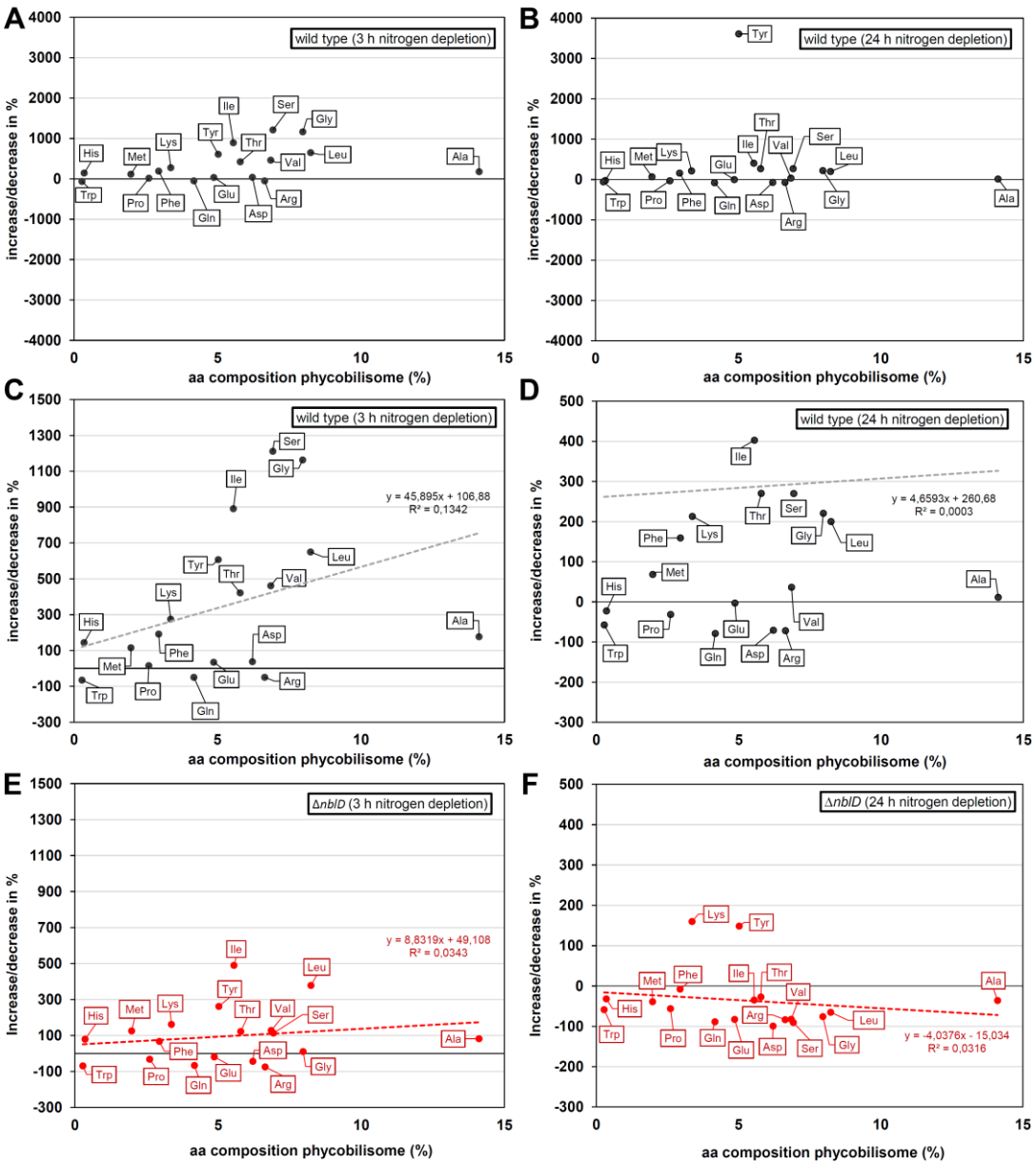

Figure 4. Phycobilisome individual amino acid (aa) composition (in %) plotted against their increase or decrease observed in relation to the initial values measured in nitrogen sufficient conditions. **A, C.** WT after 3 h; **B, D.** WT after 24 h of N limitation. **E**, **F.** Data for Δ*nblD* mutant after 3 and 24 h. Phycobilisome composition was calculated based on the structure description by Arteni et al. (33), assuming a common complex with 6 rods each with 3 hexameric phycocyanin discs and a tricylindrical allophycocyanin core. A linear trend line shows very low correlation between the variables, and a poor R-squared value indicates high variation of the data in relation to this line.

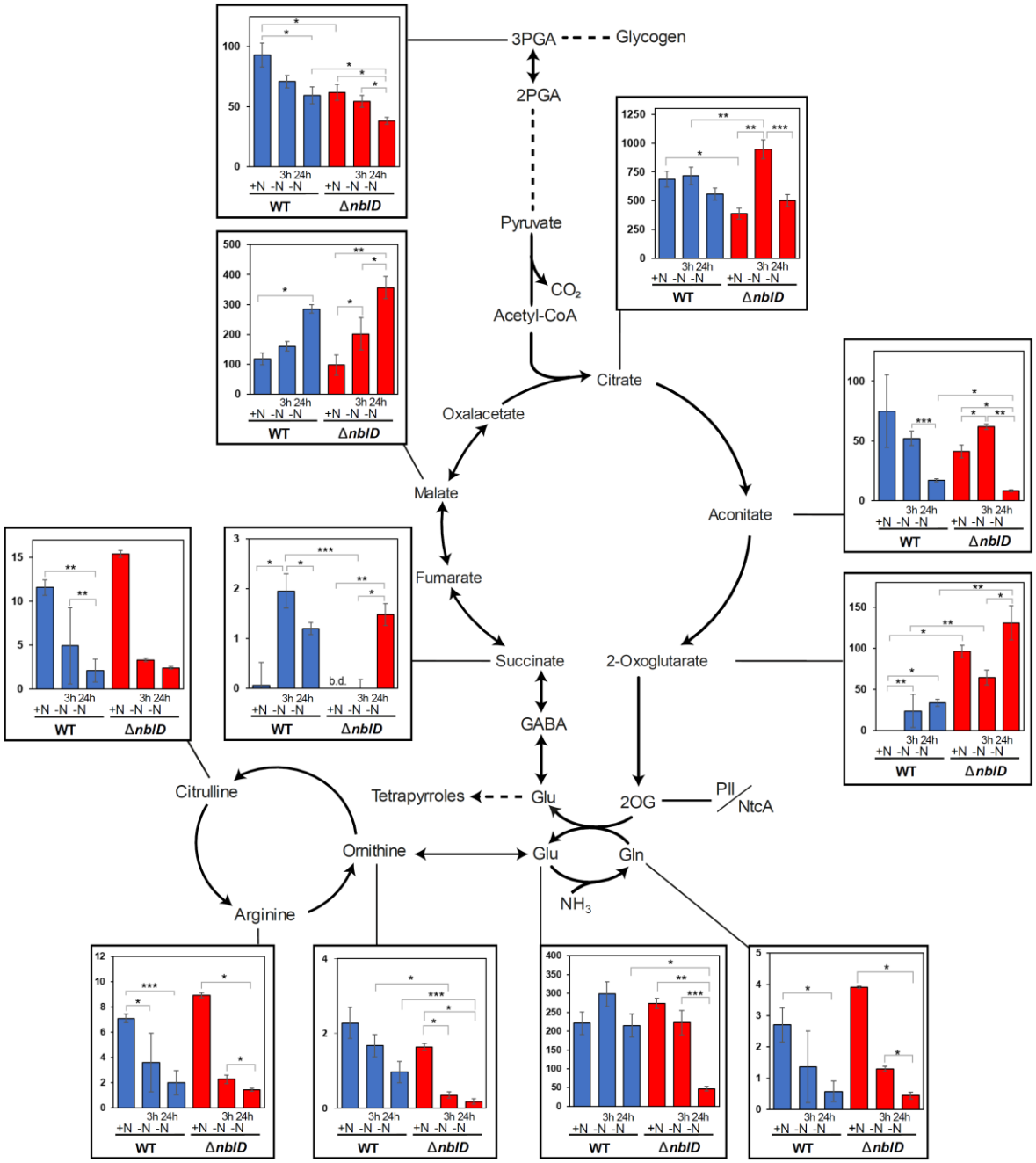

561

562 **Figure 5**. Comparison of metabolite content (in ng × ml^{-1} × OD_{750} $^{-1}$) in WT (blue) and
563 Δ*nblD* deletion mutant (red) in nitrogen replete (+N) and nitrogen deplete (-N) medium
564 after 3 h and 24 h shown alongside their biosynthetic pathways. Succinate was below
565 detection limit (b.d.) in the Δ*nblD* sample under nitrogen-replete conditions.
566 Significance was calculated with the two-sample t-test with unequal variance (Welch's
567 t-test; $p < 0.05$ = *; $p < 0.01$ = ** and $p < 0.001$ = ***) for the development in each strain
568 and between the strains at corresponding time points (details in Table S3).
569

Supplementary Tables

Table S1. LC-MS/MS data for 18 amino acids (Cyst and Asn are missing because they were below detection limit), several organic acids and GSH. Retention time (r) was individually monitored with 2 standards (line 4 and 5) and the average peak area for 1 ng (line 7), which were used to determine the ng per sample. The carnitine standard (columns E, F, G, H) was used to generate the Factor IS (internal standard), which is implemented in the normalization of the peak area for each sample.

Table S2. Total amount of all amino acids and the other soluble metabolites investigated in this study. Average, standard deviation and significance calculated by two-sample t-test (Welch's t-test) are visualized in figure 2.

Table S3. Welch's t-test (two-sided, inequal variation) for evaluating significant differences in the amino acids and organic acids between the strains and the development in the strains. Significant differences are marked in red ($p < 0.05$), boxed ($p < 0.01$) and bold italics ($p < 0.001$).